Nuclear Data for Science and Technology (1988 MITO), 399- 402, Copyright © 1988 JAERI.

IMPROVEMENTS IN NEUTRON TIME-OF-FLIGHT SPECTRA PROCESSING

G.H.R. Kegel, A. Aliyar, J.H. Chang, J.J. Egan, C.A. Horton, A. Mittler

Department of Physics
University of Lowell
Lowell, Massachusetts, 01854 USA

Abstract: At this conference Egan et. al. have reported on neutron scattering experiments on actinide nuclei with incident neutron energies in the 2 to 3 MeV range. These measurements present unique challenges because cross sections are small and excited levels are closely spaced. In this paper we review aspects of experiment design and of data reduction which assist in overcoming these difficulties (neutron scattering, actinides, elastic and inelastic cross sections, data reduction).

Introduction

Neutron scattering in the actinide region is governed by a combination of compound nucleus and direct interaction processes. The relative contribution of these two processes is fairly well established for scattering levels in ^{232}Th and ^{238}U which are part of the ground state rotational band (GSRB). At low energies the compound nucleus process prevails, reaching a maximum near 1 MeV and decreasing from there on; the direct interaction process rises slowly and steadily, it predominates at energies of about 2 MeV.

In the past we have measured neutron scattering cross sections of ^{232}Th and ^{238}U in the incident neutron energy range from 0.1 to 2 MeV covering levels of all bands [1, 2, 3] and in addition from 0.1 to 3 MeV for the GSRB[4]. Since then we have measured cross sections for levels of all bands in the 2 to 3 MeV incident neutron energy range. This paper covers some general interest aspects of instrumentation and of data reduction which refer to these measurements. A review of the experiment with a presentation and discussion of the results is given in a companion paper by J.J. Egan, A. Aliyar, C.A. Horton, G.H.R. Kegel and A. Mittler at this conference.

Experiment

In the design of the present experiment we could draw upon our earlier experience which showed that the cross sections to be measured are small, typically 50 mb, and that levels are closely spaced. These conditions lead to conflicting target thickness requirements. A thin target provides good energy resolution but poor neutron yield; a thick target has the required yield but leads to poor resolution. The target thickness eventually used presents a compromise which enabled us to determine cross section for individual levels and, in some cases, for groups of levels, while maintaining the duration of these measurements at a reasonable value.

In addition we used a NE213 scintillator with a commercial version of the Munchen [5] n-γ discrimination circuit to eliminate gamma-ray background. Time-of-flight (TOF) spectra for neutrons and for gamma rays were accumulated in separate multi-channel-analyzer (MCA) sections providing a record of n-γ discriminator performance during each run. Furthermore, the gamma peak width provided a record of overall system time resolution, not including the contribution of the neutron energy spread. This time resolution was about 500 ps throughout the series of measurements.

Data Reduction

The reduction of scattering data for many, overlapping peaks presents special problems. We overcame some of these difficulties by designing an unfolding code specifically for these studies. Our past experience has shown that the success of unfolding procedures hinges on two essentials: Peak locations and peak shapes must be accurately known. To determine these parameters we have interleaved measurements on ^{232}Th and on ^{238}U with those on natural iron. There are four prominent peaks in the iron spectrum: A gamma ray following n n'γ on ^{56}Fe, the elastic peaks of the first and the second neutron groups, and the first-neutron-group generated inelastic peak (E_x = 847 keV) of ^{56}Fe. The location of these peaks is determined using a statistically inefficient procedure [6]: A parabola is fit to the (2n + 1)-channel wide interval centered at the highest channel. From the fit residual an uncertainly of the peak location is obtained. A fit example is given in Fig. 1. From the location of the four iron peaks we can determine the scatterer- detector

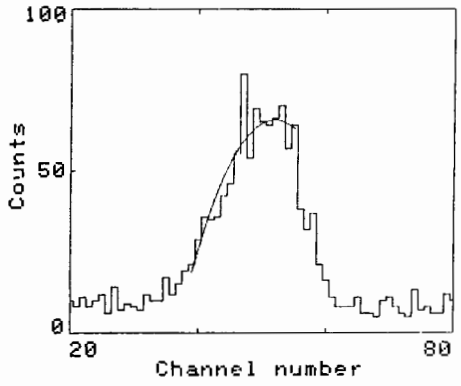

Fig. 1. A parabola fit with n = 8. The parabola fit determines the location of a poorly defined peak with an uncertainty of 1.5 channels.

distance D and the width, Δt, of the MCA time channel using appropriate weighted-fit techniques. In addition, the sharp gamma ray

identifies the arrival of the first neutron group at the target with good accuracy. Typically values of D obtained from the fit differed from the length measurements by a few millimeters; measured Δt values of 100 ps differed from fitted values by about 3 ps.

Since iron spectra were taken at the same rate as U or Th spectra any instabilities or drifts in the timing electronics would become evident immediately.

The fit results with their uncertainties were used to determine the expected locations of Th and U peaks. Fig. 2. shows the peak location uncertainties for ^{232}Th levels expressed in ps, these values are quite small.

Since the iron scatterer has a shape similar to the Th and identical the the U scatterer it is natural to use the first neutron group elastic and inelastic peaks in the TOF spectrum as shape standards. Both peaks show a small "tail" on the late side. Since the gamma profile is free of a similar tail it follows that the tails are not instrumental artifacts of the timing electronics or of the Mobley compression system of the accelerator. Rather they are assumed to be caused by a fraction of neutrons which reach the scintillator after a variable delay, possibly because they lost a small fraction of their energy in air scattering. Under these conditions we can consider the measured profile, M(t) as a sum of two terms, the first being of the same form as the prompt resolution profile P(t) and the second consisting of a convolution of P(t) with a "tail function" T(t):

$$M(t) = (1 - \varepsilon)P(t) + \varepsilon \int_{-\infty}^{t} P(u)\ T(t-u)du \qquad (1)$$

where we take T(t) as

$$T(t) = \tau^{-1} \exp(t/\tau) \qquad (2)$$

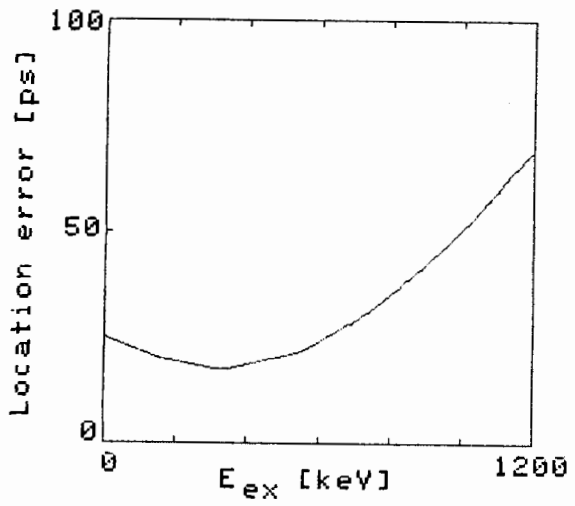

Fig. 2. Locations of inelastic neutron scattering peaks are known with an estimated error which varies from 20 to 70 ps for neutron energy losses between 0 and 1200 keV.

In our case $\varepsilon \sim .2$ and $\tau \simeq 5$ ns.

From (1) we can obtain P(t) using Fourier transform techniques. However, since is small it is simpler to solve (1) for P(t) by iteration. We write

$$P_o(t) = M(t) \qquad (3)$$

and

$$(1-\varepsilon)P_n(t) = M(t) - \varepsilon \int P_{n-1}(u)\ T(t-u)du \qquad (4)$$

Usually a single iteration is adequate to obtain P(t).

We have found that in this experiment both and are independent of energy. This allows us to use equ. 4 not only to obtain P(t), but also to process an entire scattered neutron TOF spectrum to remove tails appended to peaks; we have followed this approach. Fig. 3 shows an Fe spectrum after tail removal.

The two prominent iron peaks, the first-neutron-group elastic and inelastic scattering peaks, have shapes sufficiently different to require an energy-dependent parameterization. Several attemps have been made to obtain shape parameters. A simple Gaussian function gives an inadequate fit. Hermite functions, which may be considered as extensions of a Gaussian, worked well but required a large number (about 10) of parameters. Laguerre functions, with their build-in asymmetry appeared promising but they too required a large number of parameters. We finally found that a distorted Gaussian profile provided an adequate fit. This profile has the form

$$F(t) = \exp\left\{-B(t-t_o)^2\ (1 + C(t-t_o))\right\} \qquad (5)$$

It may be considered a Gaussian with a width parameter which is slightly time dependent, e.g. $B(1 + C(t-t_o))$. The parameter C is quite small so that $C(t-t_c)$ does not change much over the interval where F(t) differs significantly from zero. If this function is used in a computer code care must be taken not

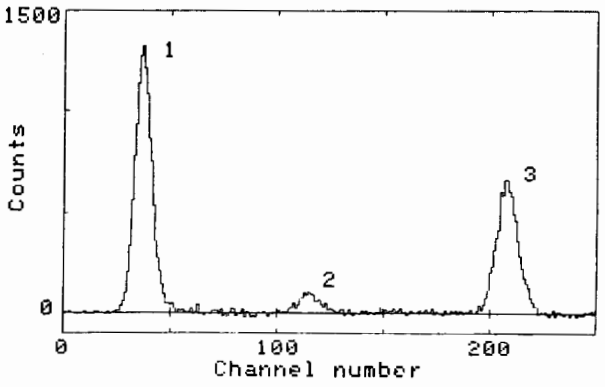

Fig. 3. An iron scattered neutron spectrum measured at an incident neutron energy of 2.4 MeV. Peaks 1, 2, and 3 represent, respectively, first neutron group elastic scattering, second neutron group elastic scattering, and first neutron group inelastic scattering on ^{56}Fe.

to let $1 + C(t-t_c)$ to become small or even negative, lest F(t) rises again.

Figure 4 shows a measured elastic iron peak and the corresponding fit by a function of the form (5). The fit residual is consistent with an a-priori estimate of the uncertainty in the number of counts in a channel. We obtain B and C parameters for both iron peaks and we use interpolation, linear in energy, to obtain B and C for other energy values, so that properly shaped profiles can be obtained for any peak in a ^{232}Th or ^{238}U scattered neutron spectrum. We have thus obtained the two essential elements, peak position and peak profiles, which we deem essential for the successful unfolding.

To unfold the scattered neutron spectrum we approximate the measured spectrum ϕ_n, where n is the channel number, by a sum of synthetic profiles F_{ni}, with i the profile number. The F_{ni} are situated at the locations in the spectrum where a peak is expected according to the respective nuclear level scheme.

$$\phi_n - \sum_j A_i F_{ni} \qquad (6)$$

The A's are determined by the usual least squares fit procedure. In matrix notation we have

$$\phi = FA \qquad (7)$$

The least squares requirement leads to

$$F^T F A = F \phi \qquad (8)$$

The matrix F^TF is square

$$F^TF = D \qquad (9)$$

and has an inverse D^{-1} so that

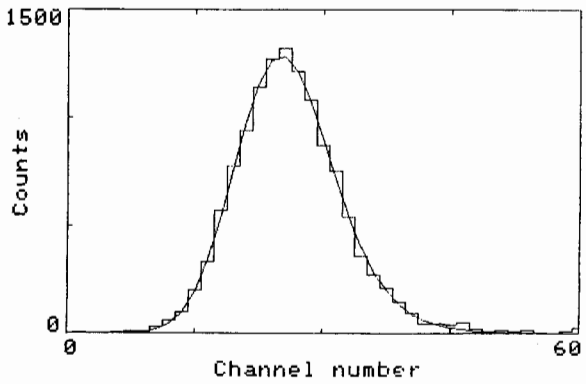

Fig. 4. A fit to a scattered neutron peak. A function of the form of equ. 5 (smooth line) has been fit to a scattered neutron peak (histogram). This is peak 1 of fig. 3.

$$A = D^{-1} F \phi \qquad (10)$$

The error of A_i, ΔA_i, is obtained using the fit residual R and the number of degrees of freedom N,

$$\Delta A_i^2 = D_{ii}^{-1} R/N \qquad (11)$$

It should be noticed that the error of the sum of two adjacent peaks, i and j, should be calculated using

$$\Delta A_{i+j}^2 = (D_{ii}^{-1} + D_{jj}^{-1} + 2D_{ij}^{-1}) R/N \qquad (12)$$

Usually this is substantially lower then either peak error because D_{ij} is negative.

Figure 5 shows a measured (0) and a fit (FA) spectrum.

The procedures outlined in this paper are embodied in several computer programs, some operator interactive, which total about 5000

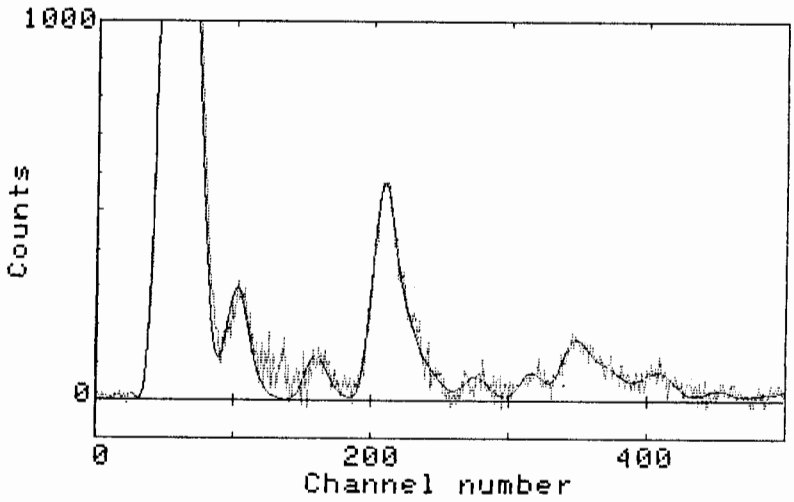

Fig. 5. A fit to a scattered neutron spectrum. A linear combination of synthetic peak profiles has been fit to a Th scattered neutron spectrum (see Egan et. al., this conference). E_n = 2.4 MeV, $\Theta = 85^o$.

line of assembler language code. A detailed description of these programs will be published elsewhere.

Fourier Techniques

Fourier techniques have been used successfully by Sloan and Woodruff[7] and by Bottcher et al.[8] to obtain data enhancements. Certainly the unfolding procedure needed to solve equ. 1 is readily performed using Fourier techniques. The same would be true for the spectrum unfolding if the shapes of the synthetic profiles F_{ni} would not be energy dependent. This is not the case however, rendering the Fourier approach less attractive. Quite generally it should be noted that the Fourier transform, most frequency domain filtering techniques, and the inverse transform all are linear operations. Hence all can be carried out in the time domain. This may not be the case if a non-linear filtering technique is used in the frequency domain, a possibility apparently unexplored, as yet.

Acknowledgements

Mr. Causen Jen and David Desimone were most helpful in the conduct of this experiment. This research was supported by a grant from the US. Department of Energy.

REFERENCES

1. J.H. Dave, J.J. Egan, G.P. Couchell, G.H.R. Kegel, A. Mittler, D.J. Pullen, W.A. Schier and E. Sheldon, Nucl. Sci. Eng. 91, 187 (1985).

2. C.A. Ciarcia, G.P. Couchell, J.J. Egan, G.H.R. Kegel, S.Q. Li, A. Mittler, D.J. Pullen, W.A. Schier and J.Q. Shao, Nucl. Sci. Eng. 91, 428 (1985).

3. J.Q. Shao, G.P. Couchell, J.J. Egan, G.H.R. Kegel, S.Q. Li, A. Mittler, D.J. Pullen, W.A. Schier and E.D. Arthur, Nucl. Sci. Eng. 92, 350 (1986)

4. L.E. Beghian, G.H.R. Kegel, T.V. Marcella, B.K. Barnes, G.P. Couchell, J.J. Egan, A. Mittler, D.J. Pullen and W.A. Schier, Nucl. Sci. Eng. 69, 191 (1979) and, G.C. Goswami, J.J. Egan, G.H.R. Kegel, A. Mittler and E. Sheldon, Nucl. Sci. Eng. (in press).

5. P. Sperr, H. Spieler, M.R. Maier and D. Evers, Nucl. Instr. Meth. 116, 55 (1974).

6. See, e.g. R.E. Evans, The Atomic Nucleus, McGraw-Hill, 1955, Appendix G.

7. W.R. Sloan and G.L. Woodruff, Nucl. Instr. Meth. 150, 235 (1978).

8. J. Bottcher, A. Feigel, E. Finckh, C. Forstner, W. Jauman, G. Schall, H. Scheuring, U. Schneidereit, K. Stauber, P. Troger and A. Weipert, Nucl. Instr. Meth. Phys. Res. 219, 369 (1984).